Analysis of the Photic Driving Effect via joint EEG and MEG data processing based on the Coupled CP decomposition

Kristina Naskovska*, *Alexey Alexandrovich Korobkov*[†], *Martin Haardt** and *Jens Haueisen* [‡]

*Communications Research Laboratory, Ilmenau University of Technology, P. O. Box 100565, D-98684 Ilmenau, Germany

Email: kristina.naskovska, martin.haardt@tu-ilmenau.de

[†]Institute of Radio Electronics and Telecommunications, Kazan National Research Technical University n.a. A.N Tupolev-KAI

[‡]Institute of Biomedical Engineering and Informatics, Ilmenau University of Technology, Ilmenau, Germany

Abstract—There are many combined signal processing applications such as the joint processing of EEG (Electroencephalogram) and MEG (Magnetoencephalogram) data that can benefit from coupled CP (Canonical Polyadic) tensor decompositions. The coupled CP decomposition jointly decomposes tensors that have at least one factor matrix in common. The C-SECSI (Coupled - Semi-Algebraic framework for approximate CP decomposition via SImultaneaous matrix diagonalization) framework provides a semi-algebraic solution for the coupled CP decomposition of noise corrupted low-rank tensors. The C-SECSI framework efficiently computes the factor matrices even in ill-posed scenarios with an adjustable complexity-accuracy trade-off. In this paper, we present a reliability test for the C-SECSI framework that can improve the model order estimation. Moreover, we analyse the photic driving effect from simultaneously recorded EEG and MEG data using the C-SECSI framework. The EEG and MEG data used in the analysis are obtained by stimulating volunteers with flickering light at different frequencies that are multiples of the individual alpha frequency of each volunteer.

I. INTRODUCTION

Tensor algebra is an efficient tool for data analysis because it preserves the multidimensional data structure and provides improved identifiability [1]. One of the most important tensor decomposition is the CP decomposition since it decomposes a given tensor into the minimum number of rank one components.

Recently, extensions to the coupled CP decomposition were proposed. The coupled CP decomposition jointly decomposes tensors that have at least one factor matrix in common. A C-SECSI framework for the efficient computation of the coupled CP decomposition was proposed in [2]. The C-SECSI framework is an extension of the SECSI framework [3], [4] for the robust estimation of coupled CP decompositions based on a truncated joint HOSVD (Higher Order Singular Value Decomposition) followed by the whole set of possible SMDs (Simultaneous Matrix Diagonalizations). Exploiting several available estimates for each of the factor matrices, the SECSI framework chooses one final estimate depending on different heuristics. Therefore, it offers a complexity-accuracy trade-off. Moreover, the C-SECSI framework is capable of jointly decomposing tensors with different SNRs (Signal to Noise Rations), i.e., a normalization with respect to the noise variance is not required [2].

The coupled CP tensor decomposition is suitable for several combined signal processing applications that can benefit from coupled tensor decompositions. Such applications include multirate sampling for array signal processing [5], [6], data fusion with heterogeneous data sets of multiple sources, i.e., social sites or review sites can be processed jointly [7] and data clustering [8]. Moreover, biomedical data analysis can benefit from coupled tensor decompositions because often EEG and MEG recordings are performed simultaneously.

IPS (Intermittent Photic Stimulation) is a stimulation of the brain by repetitive light flashes and it can induce the PD (Photic Driving) effect. IPS can cause two phenomena, a frequency entrainment and a resonance effect. Frequency entrainment is indicated by the synchronization of the individual brain rhythm with the photic stimulation frequency. The resonance effect is characterized by enlarged response amplitudes for the photic stimulation with frequencies at or close to the individual alpha frequency or half the individual alpha frequency for our study.

The PD effect is widely used to assess effects of medicaments and for diagnosis. Moreover, the PD effect is also used to study several neurophysiological diseases like Alzheimers, schizophrenia, and some forms of epilepsy. The studies of the PD effect provide evidence for the frequency selectivity of the neural oscillator network [9], [10]. The authors in [11] used the PD effect for the investigation of neurophysiological mechanisms underlying autistic symptoms. Moreover, in [12] the PD effect of epileptic patients was investigated on the basis of simultaneously recorded EEG and MEG signals. In [13], the first investigation of frequency entrainment using simultaneously recorded EEG and EMG signals during the IPS with frequency, which was adopted to the individual alpha rhythm was performed. Furthermore, in [14] a rod-driven PD effect was analysed and it was shown that strong alpha resonance phenomena exist for rod-input at stimulation frequencies around the individual alpha rhythm ($0.95 f_\alpha - 1.10 f_\alpha$) and the first subharmonic ($0.50 f_\alpha - 0.55 f_\alpha$). In [14] was shown that the rod-driven PD effect is limited by the flicker fusion threshold.

We use the following notation. Scalars are denoted either as capital or lower-case italic letters, A, a. Vectors and matrices, are denoted as bold-face capital and lower-case letters, a, A, respectively. Tensors are represented by bold-face calligraphic letters $\mathcal{A}$. The operators $||.||_F$ and $||.||_H$ denote the Frobenius norm and the higher order norm, respectively. Moreover, an n-mode product between a tensor $\mathcal{A} \in \mathbb{C}^{I_1 \times I_2 \ldots \times I_N}$ and a matrix $B \in \mathbb{C}^{J \times I_n}$ is defined as $\mathcal{A} \times_n B$, for $n = 1, 2, \ldots N$ [1]. A super-diagonal or identity N-way tensor of dimensions $R \times R \ldots \times R$ is denoted as $\mathcal{I}_{N,R}$.

The rest of the paper is organized as follows. In Section II we present the coupled CP decomposition and the proposed reliability test based on the C-SECSI framework. In Section III the data model and the construction of the tensors from the measurements data are presented. The data tensors are then analysed using the C-SECSI framework and the corresponding experimental verifications are presented in Section IV. Finally, in Section V we conclude this paper.

II. TENSOR ALGEBRA AND COUPLED CP DECOMPOSITION

If two tensors of order three, denoted by $\mathcal{X}^{(i)} \in \mathbb{C}^{M_1 \times M_2^{(i)} \times M_3^{(i)}}, i = 1, 2$ have the first factor matrix in common, then they have a coupled CP decomposition defined as

$$\mathcal{X}^{(1)} = \mathcal{I}_{3,R} \times_1 A \times_2 B^{(1)} \times_3 C^{(1)}$$
$$\mathcal{X}^{(2)} = \mathcal{I}_{3,R} \times_1 A \times_2 B^{(2)} \times_3 C^{(2)},$$

where, $A \in \mathbb{C}^{M_1 \times R}$, $B^{(i)} \in \mathbb{C}^{M_2^{(i)} \times R}$ and $C^{(i)} \in \mathbb{C}^{M_3^{(i)} \times R}$, $i = 1, 2$ are the factor matrices and R is the rank of the tensors. Moreover, the truncated coupled HOSVD, in case of noise corrupted tensors,

$$\mathcal{X}^{(1)} = \mathcal{S}^{[s],(1)} \times_1 U_1^{[s]} \times_2 U_2^{[s],(1)} \times_3 U_3^{[s],(1)} \quad (1)$$

$$\mathcal{X}^{(2)} = \mathcal{S}^{[s],(2)} \times_1 U_1^{[s]} \times_2 U_2^{[s],(2)} \times_3 U_3^{[s],(2)}, \quad (2)$$

can be calculated jointly, for the common mode using the SVD (Singular Value Decomposition),

$$\left[\ [\mathcal{X}^{(1)}]_{(1)} \quad [\mathcal{X}^{(2)}]_{(1)} \ \right] = U_1^{[s]} \cdot \Sigma_1^{[s]} \cdot V_1^{[s]H}.$$

In (1) and (2), $\mathcal{S}^{[s],(1)}$ and $\mathcal{S}^{[s],(2)} \in \mathbb{C}^{R \times R \times R}$ are the truncated core tensors and the loading matrices $U_1^{[s]} \in \mathbb{C}^{M_1 \times R}$, $U_2^{[s],(i)} \in \mathbb{C}^{M_2^{(i)} \times R}$ and $U_3^{[s],(i)} \in \mathbb{C}^{M_3^{(i)} \times R}$ have unitary columns and span the column space of the n-mode unfolding of $\mathcal{X}^{(i)}$, for $n = 1, 2, 3$ and $i = 1, 2$, respectively. Note that the matrices $U_1^{[s]}$ and A span the same column space of $[\mathcal{X}^{(1)}]_{(1)}$. Due to the fact that the tensors $\mathcal{X}^{(1)}$ and $\mathcal{X}^{(2)}$ have the factor matrix A in common, the unitary matrix $U_1^{[s]}$ should be the same for both HOSVDs.

The C-SECSI framework provides an efficient computation of the coupled CP decomposition using the joint HOSVD followed by the whole set of possible SMDs [2]. Eight initial estimates of the factor matrices are obtained, if the two tensors have one factor matrix in common, as shown in [2]. All estimates of the factor matrices, as well as an indication whether they are estimated from a transform matrix, from the diagonalized tensor, estimated via LS (Least Squeares) or a joint LS fit are summarized in Table I. From all these factor matrices

Transform Matrix	Diagonalized Tensor	LS	joint LS
$\hat{A}_{\mathrm{I}}$	$\hat{C}_{\mathrm{I}}^{(i)}$	$\hat{B}_{\mathrm{I}}^{(i)}$	-
$\hat{B}_{\mathrm{II}}^{(i)}$	$\hat{C}_{\mathrm{II}}^{(i)}$	-	$\hat{A}_{\mathrm{II}}$
$\hat{A}_{\mathrm{III}}$	$\hat{B}_{\mathrm{III}}^{(i)}$	$\hat{C}_{\mathrm{III}}^{(i)}$	-
$\hat{C}_{\mathrm{IV}}^{(i)}$	$\hat{B}_{\mathrm{IV}}^{(i)}$	-	$\hat{A}_{\mathrm{IV}}$
$\hat{B}_{\mathrm{V}}^{(i)}$	$\hat{A}_{\mathrm{V}}$	$\hat{C}_{\mathrm{V}}^{(i)}$	-
$\hat{C}_{\mathrm{VI}}^{(i)}$	$\hat{A}_{\mathrm{VI}}$	$\hat{B}_{\mathrm{VI}}^{(i)}$	-
$\hat{B}_{\mathrm{V}}^{(i)}$	$\hat{A}_{\mathrm{VII}}$	$\hat{C}_{\mathrm{VII}}^{(i)}$	-
$\hat{C}_{\mathrm{VI}}^{(i)}$	$\hat{A}_{\mathrm{VIII}}$	$\hat{B}_{\mathrm{VIII}}^{(i)}$	-

TABLE I: Estimates of the factor matrices obtained from the SMDs for tensors $\mathcal{X}^{(i)}, i = 1, 2$.

the most interesting one is the common factor matrix $\hat{A}$. It is easy to notice that the first four estimates of the common factor matrix (from $\hat{A}_{\mathrm{I}}$ to $\hat{A}_{\mathrm{IV}}$) are obtained either from the transform matrices or via joint LS fit. On the other hand, the last four estimates (from $\hat{A}_{\mathrm{V}}$ to $\hat{A}_{\mathrm{VIII}}$) are separately obtained from the diagonal elements of the diagonalized tensor. Therefore, the first four solutions are coupled and the last four are uncoupled. The final solution is then chosen for each of the tensors separately based on the minimum reconstruction error. We propose a reliability test that checks whether the same (coupled) solution is chosen for both tensors. It is based on the error between the final estimates of the coupled matrices, $\hat{A}^{(1)}$ and $\hat{A}^{(2)}$,

$$e_{\mathrm{R}} = \frac{\left\| \hat{A}^{(1)} \cdot P - A^{(2)} \right\|_{\mathrm{F}}^2}{\left\| A^{(2)} \right\|_{\mathrm{F}}^2},$$

where P is a permutation matrix of size $R \times R$ that resolves the permutation ambiguity of the CP decomposition. When the reliability error, e_{R} is very small than the reliability test has been passed. In this case, the tensors rank have been correctly chosen and the tensors are truly coupled in the common mode. If the error, e_{R} is large the

reliability test has failed which indicates that either the tensors are not coupled or the assumed tensor rank is not correct.
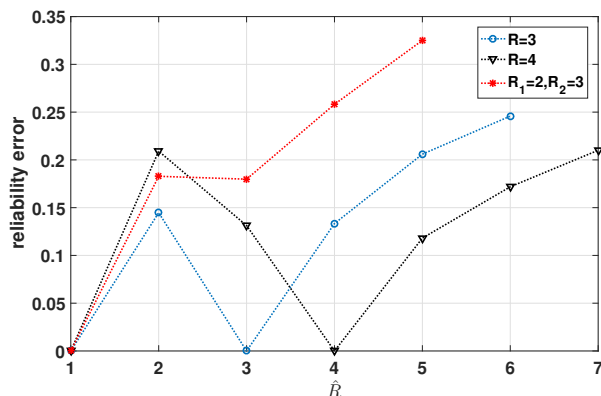

Fig. 1: Reliability error as a function of the assumed rank $\hat{R}$.

The reliability test can be used for model order estimation, i.e., rank estimation for coupled tensors. Fig. 1 visualizes the typical reliability error as a function of the assumed rank $\hat{R}$. The curves presented in Fig. 1 are results from Monte Carlo simulations with 2000 realization, for real valued tensors of dimensions $7 \times 7 \times 7$. Additionally, a white Gaussian noise was added resulting in SNR = 80 dB (Signal to Noise Ratio). The true tensor rank is indicated in the legend, whereas the assumed rank $\hat{R}$ was varied from one to seven. The reliability error has a minimum when the assumed rank equals the exact tensor rank. For the case when $R_1 = 2$ and $R_2 = 3$, i.e., when only two components are common the reliability error has local minima for both ranks. However, the reliability error will always have a minimum for $R = 1$ due to the fact that for a tensor rank equal to one the CP decomposition is equivalent to the HOSVD. Hence, only one component is estimated based on the joint HOSVD and there is only one estimate of the factor matrices. Therefore, for coupled tensors the reliability error can be used for model order estimation.

Moreover, in [2] it was shown that the C-SECSI framework unlike other ALS (Alternating Least Squares) algorithms can jointly decompose coupled tensors even if they are affected by noise with different variance. Normalization with respect to the noise variance is not required when computing the coupled CP decomposition using the C-SECSI framework.
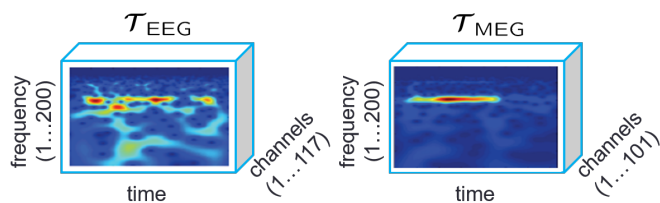
III. DATA MODEL

Fig. 2: Visualisation of the EEG and MEG data tensors, $\mathcal{T}_{\mathrm{EEG}}$ and $\mathcal{T}_{\mathrm{MEG}}$, respectively.

For the analysis presented in this paper, measurement data were used that were simultaneously recorded from 128 EEG channels and 102 MEG magnetometer channels at the Biomagnetic Center of the University Hospital in Jena, Germany. The experiment was conducted on twelve different volunteers, numbered 1 to 12 in this paper. In the

first step their individual alpha rhythm was determined during 60 seconds of resting MEG. The individual alpha frequencies, f_α were calculated by means of the averaged Fourier Transform (FT) from the occipital MEG channels. To investigate the synchronization effect of the alpha rhythm twenty different stimulation frequencies were used, from $0.40 f_\alpha$ to $2.30 f_\alpha$ with a step size of $0.05 f_\alpha$ around f_α and irregularly placed otherwise, called condition 1 to 20 in a sequel.

In addition to the usual preprocessing, a complex Morlet wavelet decomposition was used to obtain an estimate of the time-frequency distribution of the EEG and MEG signals for each channel and condition. The averaged wavelet coefficients for each of the good EEG and MEG channels were arranged as frontal slices in the third order tensor as depicted in Fig. 2. Resulting in a different tensor with dimensions frequency×time×channel for each condition, measurement and volunteer. Moreover, the frequency and the time dimension corresponds to the discretized values resulting directly from the wavelet transform. The frequency dimension contains two hundred discrete frequency values from 3 Hz until 20 Hz. The time dimension, however, varies from around 5000 ms up to 20000 ms. Therefore, there is a different number of discrete time values, depending on the corresponding condition. The variation of the length of the time dimension is due to the nature of the measurement, because each condition represents a different stimulation frequency and, therefore has a different periodicity in the time domain. Furthermore, the channel dimension represents the number of good EEG and the MEG channels, which also can vary from volunteer to volunteer and condition. Good channels are the channels that do not contain artifacts and were perfectly intact, meaning that the sensors corresponding to those channels had perfect connection during the measurement.

IV. DATA ANALYSIS

The data analysis was jointly performed for the EEG and MEG tensors based on the C-SECSI framework and for each of the conditions, respectively. It was assumed that the frequency mode is common for both the EEG and MEG tensor.
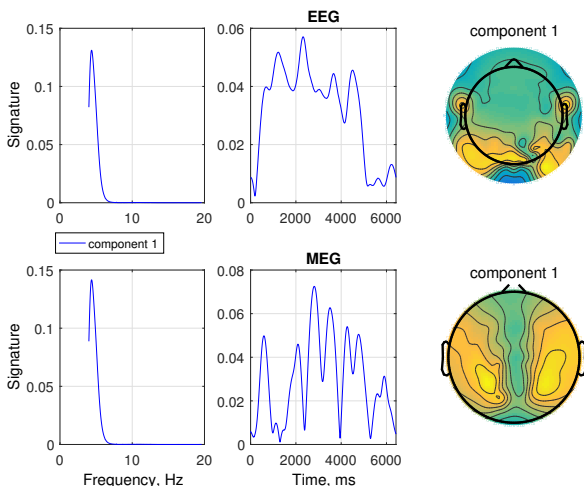

Fig. 3: Time, frequency and channel signature for volunteer 5, stimulation frequency of 4.28 Hz and tensor rank 1.

Before the computation of the coupled CP decomposition, each of the tensors was normalized to a norm one according to

$$\mathcal{T}_{N,EEG} = \frac{\mathcal{T}_{EEG}}{||\mathcal{T}_{EEG}||_H} \quad \text{and} \quad \mathcal{T}_{N,MEG} = \frac{\mathcal{T}_{MEG}}{||\mathcal{T}_{MEG}||_H}.$$
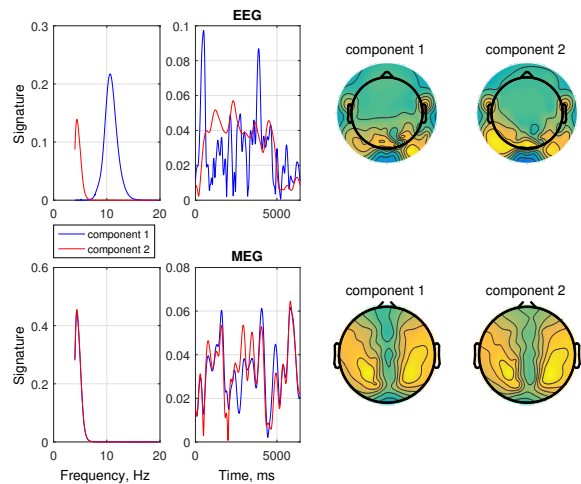

Fig. 4: Time, frequency and channel signature for volunteer 5, stimulation frequency of 4.28 Hz and tensor rank 2.
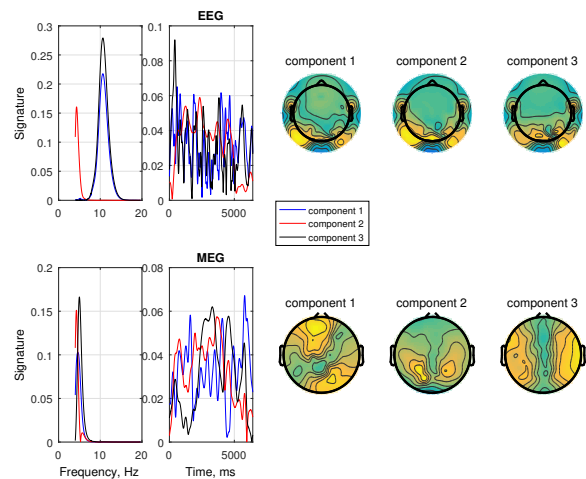

Fig. 5: Time, frequency and channel signature for volunteer 5, stimulation frequency of 4.28 Hz and tensor rank 3.

In [2] was shown that the C-SECSI framework does not require normalization with respect to the noise variance. However, the normalization to norm one tensors is necessary here due to the different dimensionality of the EEG and MEG tensors values (micro Volt and femto Tesla).

For each of the conditions, the coupled CP decomposition is computed for an assumed rank, $\hat{R} = 1, 2, 3$. In the rest of this section, we present some of the typical results that have been encountered during the analysis. In the following figures we present the frequency, time and channels signatures for volunteer 5. The frequency, time, and channel signatures represent the corresponding factor matrices of each tensor dimension.

In Fig. 3, Fig. 4 and Fig. 5 the frequency, time and a topographic plot of the channel signature for the first condition are presented, for $\hat{R} = 1$, $\hat{R} = 2$ and $\hat{R} = 3$, respectively. For an assumed rank $\hat{R} = 1$, Fig. 3 shows that the dominant component for both the EEG and MEG data is the component with a frequency equal to the stimulation frequency. Note that by using the time component the

FD effect can be analyzed further. The topographic visualization of the channels signature depicts the occipital area where the PD effect was expected to occur. Taking into account Fig. 4 and Fig. 5, and comparing the resulting frequency signatures for EEG and MEG it is obvious that they are not identical, although the frequency dimension was taken as the common mode. Therefore, it can be concluded that the reliability test has failed, indicating that the assumed rank is not correct. Moreover, the reliability error for condition one is depicted in Fig. 9 as a function of the assumed rank. The reliability error, as introduced in Section II, indicates the error between the estimated coupled matrices, up to a permutation and scaling ambiguity. For this analysis we have assumed that the EEG and MEG tensors have common frequency signatures. Therefore, the reliability error is the error between the corresponding EEG and MEG frequency signatures. For condition 1, based on the minimum of the reliability error presented in Fig. 9, we see that the EEG and the MEG tensor have only one common component. However, it cannot be excluded that one of the tensors has a higher rank. Additionally, if we compare each of the two components for the EEG and the MEG with one another as depicted in Fig. 4, we see that the second component is common for both tensors. Therefore, it can be concluded that for condition one, the EEG data and the MEG data have ranks $R_{\text{EEG}} = 2$ and $R_{\text{MEG}} = 1$, respectively. One of the components is common and corresponds to the stimulation frequency, whereas the second component for the EEG corresponds to the alpha frequency of the volunteer 5.
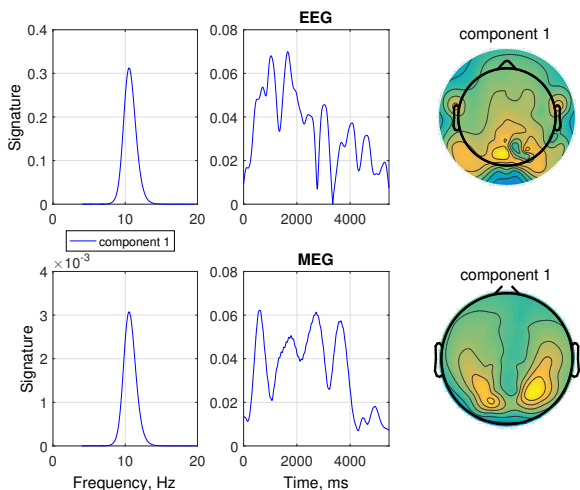

Fig. 6: Time, frequency and channel signature for volunteer 5, stimulation frequency of 5.35 Hz and tensor rank 1.

Moreover, in Fig. 6, Fig. 7 and Fig. 8 the frequency, time and channels signatures for subject 5, condition 3 corresponding to stimulation frequency of 5.53 Hz are presented. The three figures depict different assumed ranks, $\hat{R} = 1, 2, 3$. The reliability error for condition 3 is also depicted in Fig. 9. For condition 3, both the EEG and the MEG tensor have two components with a common frequency signature. The two components correspond to the stimulation and the alpha frequency, respectively.

In Fig. 9, the reliability error for the above presented conditions, condition 1 and condition 3 is visualized. The reliability test is a powerful tool for model order estimation of coupled tensors. If both tensors have exactly the same rank $R_{\text{EEG}} = R_{\text{MEG}}$ the C-SECSI framework together with the reliability test can reveal the exact
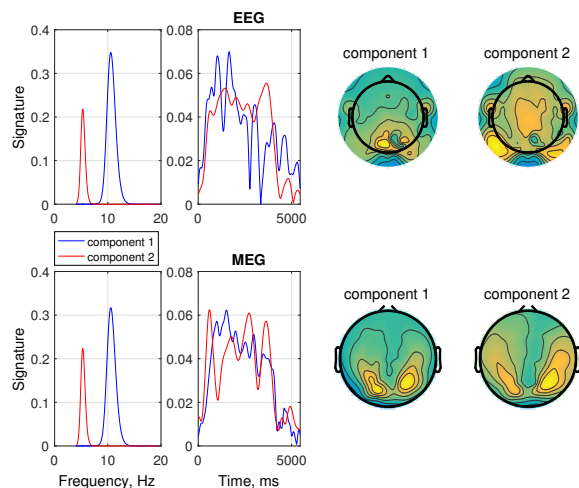

Fig. 7: Time, frequency and channel signature for volunteer 5, stimulation frequency of 5.35 Hz and tensor rank 2.
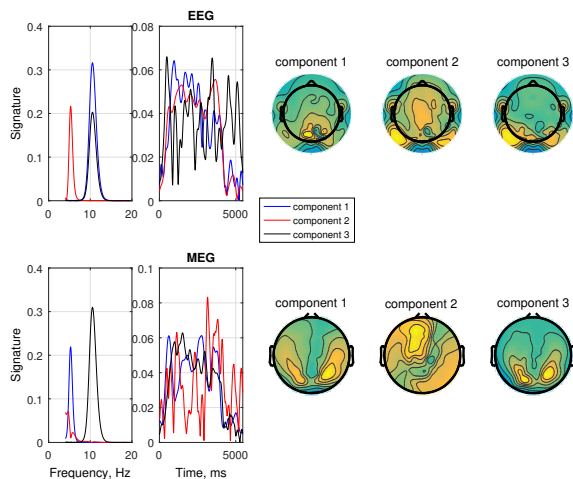

Fig. 8: Time, frequency and channel signature for volunteer 5, stimulation frequency of 5.35 Hz and tensor rank 3.

tensors rank and the underlying parallel components. Ambiguity arises only in cases as in the previously presented condition 1. Based on the reliability test alone we cannot determine whether the two tensors have rank one, or if they have only one common component and different (dominant) ranks. Therefore, for condition 1 additionally the reconstruction error has to be calculated.

Furthermore, the results obtained from the joint analysis of the EEG and the MEG data for volunteer 5 and condition one to eleven are summarized in Table II and Table III, respectively. Moreover, in both tables the resulting frequencies for tensor rank equal to 1 and 2 are presented. The higher ranks are omitted, because in none of the investigated cases the rank for both EEG and MEG was higher than two. For most of the investigated cases, the EEG measurement appeared to be rank two, whereas the MEG measurement was rank one. If two components are present, usually one of the components represents the stimulation frequency. On the other hand, the second component is not necessarily common for the EEG and the MEG measurements.
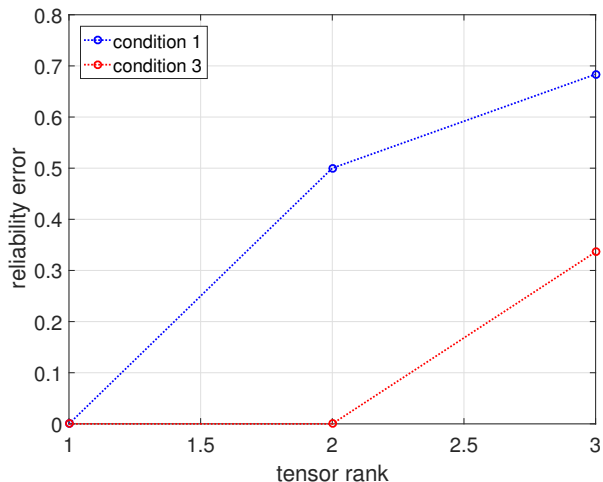
Fig. 9: Reliability error between the common frequency signatures as a function of the assumed tensor rank.

Condition	Stim. frequency	Rank 1	Rank 2	
			comp.1	comp.2
1	4.28 Hz	4.367 Hz	4.367 Hz	10.64 Hz
2	4.82 Hz	4.808 Hz	4.831 Hz	9.804 Hz
3	5.35 Hz	10.53 Hz	5.291 Hz	10.53 Hz
4	5.89 Hz	5.814 Hz	4.926 Hz	5.814 Hz
5	6.42 Hz	6.369 Hz	4.739 Hz	6.369 Hz
6	7.49 Hz	7.353 Hz	4.762 Hz	7.353 Hz
7	8.56 Hz	8.621 Hz	8.621 Hz	10.2 Hz
8	9.63 Hz	9.615 Hz	9.524 Hz	10.99 Hz
9	10.17 Hz	10.1 Hz	10.1 Hz	10.1 Hz
10	10.7 Hz	10.42 Hz	10.2 Hz	10.31 Hz
11	11.24 Hz	10.64 Hz	9.804 Hz	10.64 Hz

TABLE II: Frequencies obtained from the joint analysis for the EEG data, volunteer 5, condition one to eleven, and tensor rank one and two.

Finally, the photic driving effect for both EEG and MEG, as expected, was noticeable for the stimulation frequencies around $0.5f_\alpha$ and f_α, i.e., condition 3 and 10. For the stimulation frequency around $0.5f_\alpha$ there were two clear components corresponding to $0.5f_\alpha$ and f_α. On the other hand, for stimulation frequencies around f_α there was only one component present in the EEG, corresponding to f_α and a second component around $0.5f_\alpha$ for the MEG.

Condition	Stim. frequency	Rank 1	Rank 2	
			comp.1	comp.2
1	4.28 Hz	4.367 Hz	4.367 Hz	4.367 Hz
2	4.82 Hz	4.808 Hz	4.808 Hz	9.804 Hz
3	5.35 Hz	10.53 Hz	5.291 Hz	10.53 Hz
4	5.89 Hz	5.814 Hz	4.902 Hz	5.848 Hz
5	6.42 Hz	6.369 Hz	4.739 Hz	6.369 Hz
6	7.49 Hz	7.353 Hz	4.762 Hz	7.353 Hz
7	8.56 Hz	8.621 Hz	4.878 Hz	8.621 Hz
8	9.63 Hz	9.615 Hz	4.854 Hz	9.615 Hz
9	10.17 Hz	10.1 Hz	4.831 Hz	10.1 Hz
10	10.7 Hz	10.42 Hz	4.651 Hz	10.53 Hz
11	11.24 Hz	10.64 Hz	4.762 Hz	10.64 Hz

TABLE III: Frequencies obtained from the joint analysis for the MEG data, volunteer 5, condition one to eleven, and tensor rank one and two.

V. CONCLUSION

Coupled SECSI (C-SECSI) provides a robust framework for the efficient computation of the coupled CP tensor decomposition in many challenging scenarios. For instance, the C-SECSI framework is suitable for processing simultaneously obtained EEG and MEG measurements. In this paper, we have presented the analysis of the photic driving effect using the C-SECSI framework. We have shown that based on a new reliability test, the model order estimation for coupled tensors can be improved. Moreover, the EEG and MEG tensor have at least one common frequency signature corresponding to the stimulation frequency. However, they do not necessarily have the same (dominant) tensor rank. To this end, tensors that have a common mode but contain different parameters can be jointly decomposed using the C-SECSI framework. Moreover, the robustness of the C-SECSI framework allows the computation of the coupled CP decomposition of low rank tensors that might even have different ranks. Using the new reliability test, the rank of the coupled decomposition can be controlled.

REFERENCES

[1] T. Kolda and B. Bader, "Tensor decompositions and applications," *SIAM Review*, vol. 51, pp. 455–500, 2009.

[2] K. Naskovska and M. Haardt, "Extension of the semi-algebraic framework for approximate CP decompositions via simultaneous matrix diagonalization to the efficient calculation of coupled CP decompositions," *in Proc. of 50th Asilomar Conf. on Signals, Systems, and Computers*, Nov. 2016.

[3] F. Roemer and M. Haardt, "A semi-algebraic framework for approximate CP decomposition via simultaneous matrix diagonalization (SECSI)," *Signal Processing*, vol. 93, pp. 2722–2738, September 2013.

[4] ——, "A closed-form solution for parallel factor (PARAFAC) analysis," *Proc. IEEE Int. Con. on Acoustics, Speech and Sig. Proc. (ICASSP 2008)*, pp. 2365–2368, April 2008.

[5] M. Sorensen and L. D. Lathauwer, "Multidimensional harmonic retrieval via coupled canonical polyadic decomposition — part I: Model and identifiability," *IEEE Transactions on Signal Processing*, (accepted) 2016.

[6] ——, "Multidimensional harmonic retrieval via coupled canonical polyadic decomposition — part II: Algorithm and multirate sampling," *IEEE Transactions on Signal Processing*, (accepted) 2016.

[7] E. Acar, T. G. Kolda, and D. M. Dunlavy, "All-at-once optimization for coupled matrix and tensor factorizations," *MLG11: Proceedings of Mining and Learning with Graphs*, August 2011.

[8] E. Acar, R.Bro, and A. Smidle, "Data fusion in metabolomics using coupled matrix and tensor factorization," *Proceedings of IEEE*, vol. 103, pp. 1602 – 1620, August 2015.

[9] N. N. Danilova, "Images of working memory processes by localization of activated frequency selective EEG generators," *Psychology in Russia State of the Art. Scientific yearbook / Ed. by Yu.P. Zinchenko, V.F. Petrenko*, vol. 3, pp. 287 – 300, 2010.

[10] A. Notbohm, J. Kurths, and C. Herrmann, "Modification of brain oscillations via rhythmic light stimulation provides evidence for entrainment but not for superposition of event-related responses," *Front. Hum. Neurosci*, vol. 10, 2016.

[11] V. V. Lazarev, A. Pontes, and L. de Azevedo, "EEG photic driving: Right-hemisphere reactivity deficit in childhood autism. a pilot study," *International Journal of Psychophysiology*, vol. 71, pp. 177 – 183, 2009.

[12] S. Kalitzin, J. Parra, D. N. V. Lopes, and F. H. da Silva, "Enhancement of phase clustering in the EEG/MEG gamma frequency band anticipates transitions to paroxysmal epileptic form activity in pileptic patients with known visual sensitivity," *IEEE Trans. Biomed. Eng*, vol. 49, pp. 1279 – 1286, 2002.

[13] K. Schwab, C. Ligges, T. Jungmann, B. Hilgenfeld, J. Haueisen, and H. Witte, "Alpha entrainment in human electroencephalogram and magnetoencephalogram recordings," *Neuroreport*, vol. 17, pp. 1829 – 1833, 2006.

[14] C. Salchow, D. Strohmeier, S. Klee, D. Jannek, K. Schiecke, H. Witte, A. Nehorai, and J. Haueisen, "Rod driven frequency entrainment and resonance phenomena," *Front. Hum. Neurosci*, vol. 10, 2016.